Electronic Supplementary Material (ESI) for Nanoscale.

Supplementary Information

Heteromeric Guanosine (G)-Quadruplex Derived Antenna Modules with Directional Energy Transfer

Mohammad Amin Zarandi,[a] Pravin Pathak,[a] Noah Beltrami,[a] Jada N. Walker,[b] Fengqi Zhang,[a] Jennifer S. Brodbelt,[b] Russell Schmehl[a] and Janarthanan Jayawickramarajah*[a]

[a]Department of Chemistry, Tulane University, New Orleans, LA, 70118, USA.

[b]Department of Chemistry, The University of Texas at Austin, Austin, TX 78712, USA.

Table of contents

S1. Materials and Methods

S1.1. Materials

The precursor oligodeoxynucleotide (ODN) sequences were synthesized by the W. M. Keck Foundation Biotechnology Resource Laboratory located at Yale University, using standard automated solid-phase synthesis. 5'-Fluorescein Phosphoramidites and Fluorescein-dT Phosphoramidites used to prepare these ODNs were purchased from Glen Research. Unless otherwise noted, all chemicals and solvents were purchased from Sigma-Aldrich or Fisher Scientific and used without further purification.

S1.2. RP-HPLC conditions

All ODNs were directly purified with RP-HPLC after solid-phase synthesis. RP-HPLC purification was achieved using a Varian Prostar HPLC system, equipped with a Polymer Laboratories 100 Å 5 μm 4.6 × 250 mm PLRP-S reverse-phase column. The column was maintained at 65 °C for all runs. The flow rate was set at 1 mL/min. A gradient composed of two solvents (solvent A is 0.1 M TEAA (aq) in 5% acetonitrile and solvent B is 100% acetonitrile) was used. Absorption wavelengths were set at 260 nm (DNA absorption) and 490 nm (Fluorescein absorption).

S1.3. MALDI-TOF mass spectrometry

RP-HPLC purified samples were dried with a vacuum concentrator (Savant SpeedVac SPD 140DDA) and then re-dissolved in ultrapure water. MALDI-TOF spectra were recorded on a Bruker Daltonics Autoflex III matrix-assisted laser desorption ionization-time-of-flight mass spectrometer (MALDI-TOF MS) or a Bruker Daltonics Autoflex Speed MALDI TOF/TOF, with positive ion and linear detection modes. The matrix used was 3-hydroxypicolinic acid for all ODNs (Figures S9-S14).

S1.4. Electrospray ionization mass spectrometry (ESI-MS)

Pre-annealed solutions containing 10 μM ODN sequences in 100 mM potassium phosphate buffer (e.g., ODNs 1+2) were buffer exchanged into 150 mM ammonium acetate using a Micro Bio-Spin P-6 Gel Column (Bio-Rad Laboratories Inc.; Hercules, CA). Approximately 2-5 μL of sample was loaded into a Au/Pd-coated borosilicate static emitter and subjected to nano-electrospray ionization using a source voltage of 0.75 kV. All ions were mass analyzed in the negative ion mode on a Q Exactive HF-X Orbitrap Mass Spectrometer (Thermo Fisher Scientific; Bremen, Germany) that was modified with a 193 nm excimer laser to allow ultraviolet photodissociation (UVPD) in the HCD cell. The mass spectrometer was operated in high mass range (HMR) mode with a trapping gas setting of 1 (a.u.). In-source collision induced dissociation (CID), with voltages ranging from 10-130 V, was applied to enhance the desolvation and detection of ions. Mass spectra were collected using a resolving power of 240,000 at *m/z* 200, an

automatic gain control (AGC) target of 1e6 charges, and a lowered heated capillary temperature of 90 °C to preserve non-covalent quadruplexes. Representing 200 spectral averages, each spectrum was deconvoluted using the Xtract algorithm in FreeStyle version 1.8 (Thermo Fisher Scientific) which fits a distribution that corresponds to the nucleotide isotope table. The following deconvolution parameters were applied: signal-to-noise threshold: 3; fit factor: 80%; remainder threshold: 25%. All mass spectra were interpreted and annotated manually with the aid of Mongo Oligo Mass Calculator v2.06.

S1.5. UV-vis spectroscopy

The concentration of purified ODNs was quantified on the basis of their UV-vis absorption at 260 nm at 75°C for all ODNs, and their molar extinction coefficients were obtained from IDT-DNA. UV-vis studies were undertaken using a Hewlett-Packard 8452A diode array spectrophotometer.

S1.6. CD spectroscopy

ODN solutions were prepared in 100 mM potassium phosphate buffer (pH 7.3) (termed as "K^+ buffer"), heated at 95°C for 10 minutes in a Gene Mate mini dry bath, annealed at RT for 6 hours and then kept at 4°C for 72 hours before any experiments. Circular dichroism spectra were obtained on an Olis RSM 1000 CD using a cylindrical cuvette with 1 mm path length. All experiments were conducted with 300 µL solution of ODNs (20 µM, single-strand conc.) in K^+ buffer.

S1.7. Steady-State Fluorescence spectroscopy

Steady-State fluorescence studies were carried out using a BioTek Cytation 5 Cell Imaging Multimode Reader. All fluorescence studies were conducted at room temperature by applying 50 µL sample in Costar- 96 well standard black plates. All fluorescence profiles for each system were normalized to the fluorescein emission maximum of **GqI-GqIII** (520 nm). Fluorescence profiles were smoothed by applying a Savitzky-Golay filter**.**

S2. Procedure for Formation and Isolation of Heteromeric G-Quadruplexes

S2.1. Preparation of G-quadruplex assemblies

*Assembly **GqI***

50 µM solution of ODN1 and ODN2 were prepared in K^+ buffer separately and were mixed in a 1:1 ratio in an Eppendorf tube. In the next step, the solution was heated in a dry bath at 95°C for 10 minutes and then removed from the dry bath and kept at room temperature for 6 hours (for complete annealing). Finally, the Eppendorf tube was transferred to the fridge and was kept at 4°C for 72 hours.

*Assembly **GqII***

A similar procedure for preparation of assembly **GqI** was used. Here, 50 μM solution of ODN3 and ODN4 in K^+ buffer was mixed and annealed together (See Figure S17-S18).

*Assembly **GqIII***

A similar procedure for preparation of assembly **GqI** was used. Here, 50 μM solution of ODN1 and ODN5 in K^+ buffer was mixed and annealed together (See Figure S19-S20).

S2.2. PAGE studies

S2.2.1. General information

Non-denaturing polyacrylamide gel electrophoresis was conducted using an Invitrogen XCell SureLock Mini-Cell electrophoresis system. Precast Novex™ TBE gels (20%) purchased from Invitrogen were used for the gel studies. All gel electrophoresis were performed in TBE buffer containing 33 mM KCl. A 5 μL portion of 5 μM solution (in K^+ buffer; unless otherwise stated) of ODNs was applied to the gel (along with 1 μL of 6x DNA loading dye) and was run at RT for 150 minutes at 90V. After electrophoresis, the gel was visualized by SYBR Safe staining in a Bio-Rad ChemiDoc Imaging system.

S2.2.2. Isolation of G-quadruplex with one toehold

Preparation and extraction of each heteromeric G-quadruplex assembly with one overhang was conducted following this procedure. The procedure was conducted under minimum light in a dark room (to minimize the effect of light on the dyes). A 50 μM annealed solution of two oligonucleotides was applied to the gel and was run for 150 minutes at 90V. At the end of each gel electrophoresis, the gel was separated from the cassette and placed on a dark reader transilluminator without using any DNA gel stain. The fluorescent (as a result of the fluorescein dyes) gel bands were visualized under visible blue light as the excitation source (420-500 nm) and each band was incised using a new razor blade. Next, each incised band was transferred to an Eppendorf tube and the gel band was crushed inside the tube, using a spatula. Subsequently, the K^+ buffer was added to each Eppendorf tube, stored at 4°C for 48 hours and vortexed every few hours to maximize DNA extraction. After 48 hours, each tube was centrifuged twice at 10000 rcf and the supernatant was collected, concentrated, and stored at 4°C for the next steps.

S2.3. Procedure for formation of 1:1 complex of heteromeric (G)-quadruplex and EA single strand

S2.3.1. Estimation of concentration using fluorescence calibration curves

A 1:1 complex of each heteromeric G-quadruplex assembly and the TAMRA acceptor dye containing single strand (**EA**) that is complementary to the overhang region of the quadruplexes (and whose concentration can be accurately measured) was prepared in two steps. In the first step, the concentration range of each assembly was estimated via fluorescence calibration curves using a Multimode Reader. In the second step, an energy transfer titration study was conducted to determine a 1:1 complex formation for each heteromeric G-quadruplex assembly.

First, the concentration of each single stranded ODN in ultrapure water was measured using UV-vis at 260 nm at 75°C. Next, a 10 μM stock solution of each ODN was prepared in K^+ buffer (but not annealed to not initiate quadruplexes formation). Finally, 4 separate samples with concentration of 50, 100, 150 and 200 nM were prepared from the stock solution of each ODN. The fluorescence intensity of each sample was measured using a Multimode Reader and calibration curve was developed for each ODN in the concentration range of 0-200 nM (Figure S1-S4).

After isolation, extraction, and purification of each assembly (**GqI-GqIII**) from the gel, the fluorescence intensity of each assembly was measured using the Multimode reader. From these fluorescence intensity measurements, the corresponding concentration of the two ODN components of that assembly (for example ODNs **1** and **2** for **GqI**) was estimated using the two respective calibration curves for the single stranded ODNs. Finally, the concentration of each assembly was estimated based on the following equations:

(a) For **GqI**, the average concentration of the heteromeric single strands (each containing two fluorescein dyes) were calculated based on the weighted concentration of **1** and **2** in a 1/4 to 3/4 ratio (because the overall fluorescence intensity of **GqI** containing solution is derived from one part **1** and three parts **2**). Then, to calculate the concentration of the **GqI** assembly, the averaged single strand concentration was divided by 4.

$$[GqI] = \left(\frac{(3 \times [ODN2]) + [ODN1]}{4}\right)\Big/4$$

(eq. S1)

(b) For **GqII**, the average concentration of the heteromeric single strands (each containing one fluorescein dye) were calculated based on the weighted concentration of **3** and **4** in a 1/4 to 3/4 ratio (because the overall fluorescence intensity of **GqII** containing solution is derived from one part **3** and three parts **4**). Then, to calculate the concentration of the **GqII** assembly, the averaged single strand concentration was divided by 4.

$$[GqII] = \left(\frac{(3 \times [ODN4]) + [ODN3]}{4}\right)\Big/4$$

(eq. S2)

(c) Since **GqIII** is composed of only one strand of ODN 1 (that is decorated with two fluorescein dyes) and 3 strands of ODN 5 (that has no fluorescein handles), the concentration of **GqIII** was directly estimated using only the calibration curve of ODN1.

$$[GqIII] = [ODN1] \qquad \text{(eq. S3)}$$

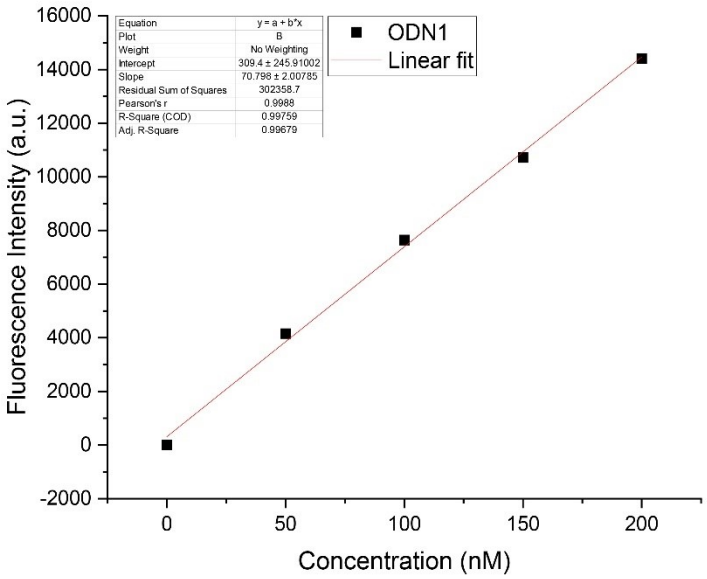

Figure S1. Fluorescence calibration curve of ODN1 in range of 0-200 nM. Data were fitted using linear fit function in Origin Pro (R-square:0.998).

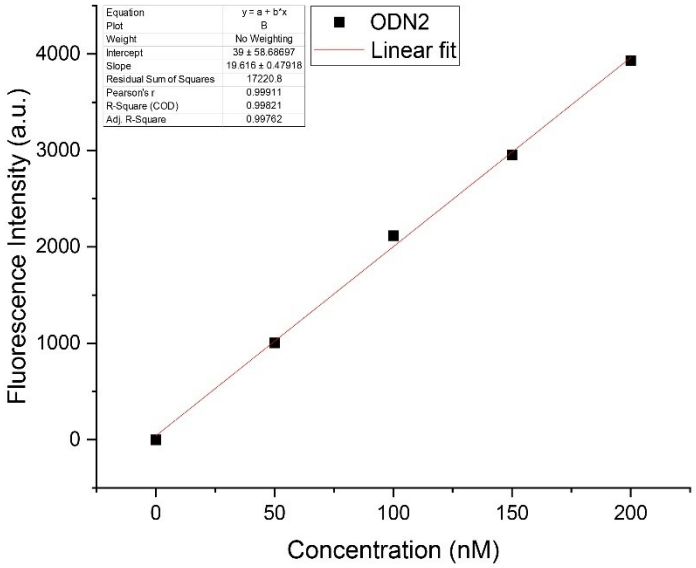

Figure S2. Fluorescence calibration curve of ODN2 in range of 0-200 nM. Data were fitted using linear fit function in Origin Pro (R-square:0.998).

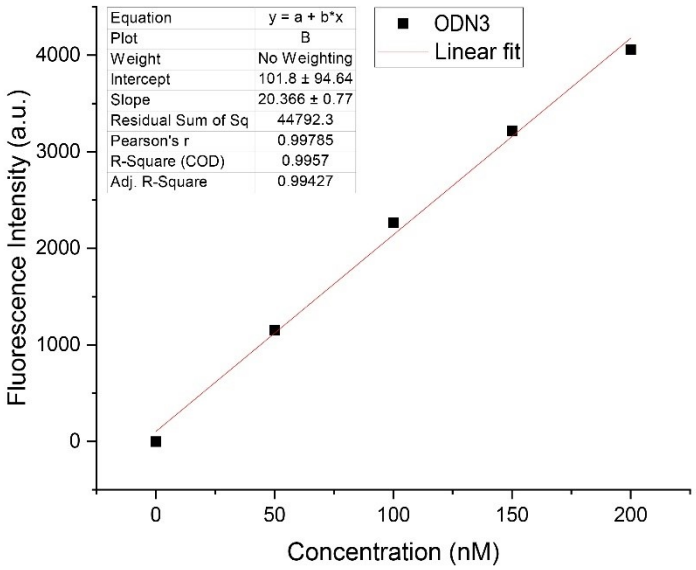

Figure S3. Fluorescence calibration curve of ODN3 in range of 0-200 nM. Data were fitted using linear fit function in Origin Pro (R-square:0.996).

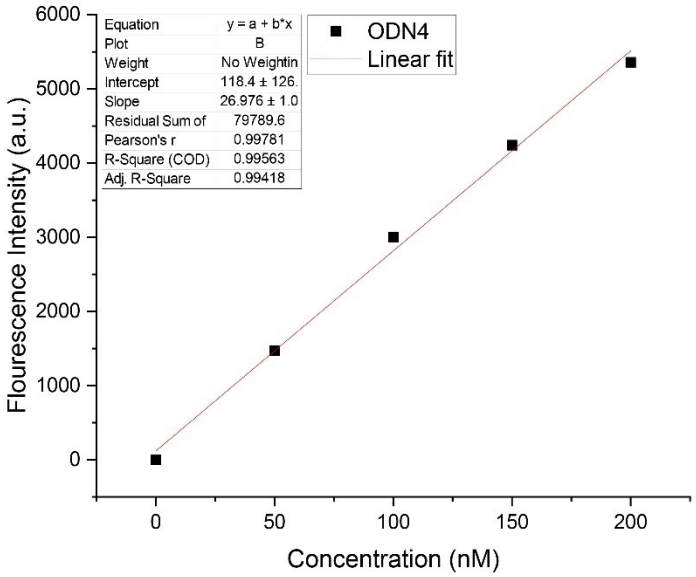

Figure S4. Fluorescence calibration curve of ODN4 in range of 0-200 nM. Data were fitted using linear fit function in Origin Pro (R-square:0.996).

S2.3.2. Titration study based on acceptor emission intensity

In the next step, a 15 nM concentration of each heteromeric quadruplex was prepared using the protocol and fluorescence calibration curves described in section S2.3.1. In order to form a 1:1 complex of each heteromeric quadruplex and **EA** single strand, a second step was conducted. Here **EA** single strand was titrated into the solution of each assembly (**GqI-GqIII**). The hybridization of quadruplexes **GqI-GqIII** with **EA** was then monitored via fluorescence. Specifically, at each aliquot of **EA** added, the fluorescein donors of **GqI-GqIII** were excited and emission from the TAMRA acceptor was measured until the emission reached a maximum fluorescence value (e.g., Figure S5 for **GqI**). At this value, it was assumed that a 1:1 complex was fully formed. All the photophysical studies for each system were based on 1:1 complex derived from this method.

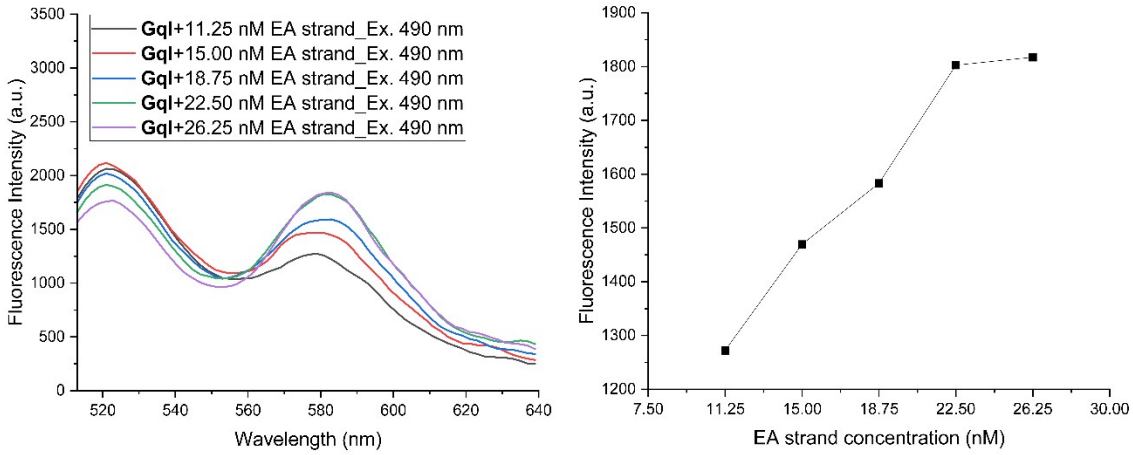

Figure S5. Fluorescence titration study of **EA** to **GqI**. The 1:1 complex of **GqI:EA** was formed at 22.5 nM. **left:** Fluorescence spectrum 513-640 nm with excitation at 490 nm; **right:** Fluorescence emissions at 580 nm.

S3. Quantum yield studies

S3.1. Quantum yield equations for GqI-GqIII

6-carboxyfluorescein was selected as a reference dye due to the structural resemblance to the conjugated 6-FAM dyes used on the ODNs for this study. Unfortunately, the heteromeric **GqI-GqIII** quadruplexes could not be used directly for this study since the concentrations required were too high as these were isolated from PAGE with nM concentrations. Thus, for all the heteromeric assemblies **(GqI-GqIII)**, the closest homomeric G-quadruplex species or the closest single-strand with same number and position of fluorescein dyes were selected for quantum yield calculations.

For assembly **GqI**, the quantum yield of assemblies $\mathbf{1}_4$ and $\mathbf{2}_4$ were first calculated. **GqI**, $\mathbf{1}_4$ and $\mathbf{2}_4$ have the same number and position of fluorescein dyes with different number of overhang region (Figure S6A). Therefore, the quantum yield of $\mathbf{1}_4$ and $\mathbf{2}_4$ were averaged by the ratio of 1 to 3 (equation S4).

$$QY_{GqI} \simeq \frac{3 \times QY_{(2_4)} + QY_{(1_4)}}{4}$$

(eq. S4)

For assembly **GqII**, the same reasoning was utilized. Here, the average quantum yield of assemblies $\mathbf{3}_4$ and $\mathbf{4}_4$ were calculated and averaged by the ratio of 1 to 3 (Figure S6B).

$$QY_{GqII} \simeq \frac{3 \times QY_{(4_4)} + QY_{(3_4)}}{4}$$ (eq. S5)

For assembly **GqIII** containing one fluorescein dye at the 5' end and one fluorescein dye at the 3' end, the quantum yield of single-stranded ODN3 was calculated and was assumed to be the quantum yield of **GqIII** (Figure S6C and equation S6).

$$QY_{GqIII} \simeq QY_{ODN1}$$ (eq. S6)

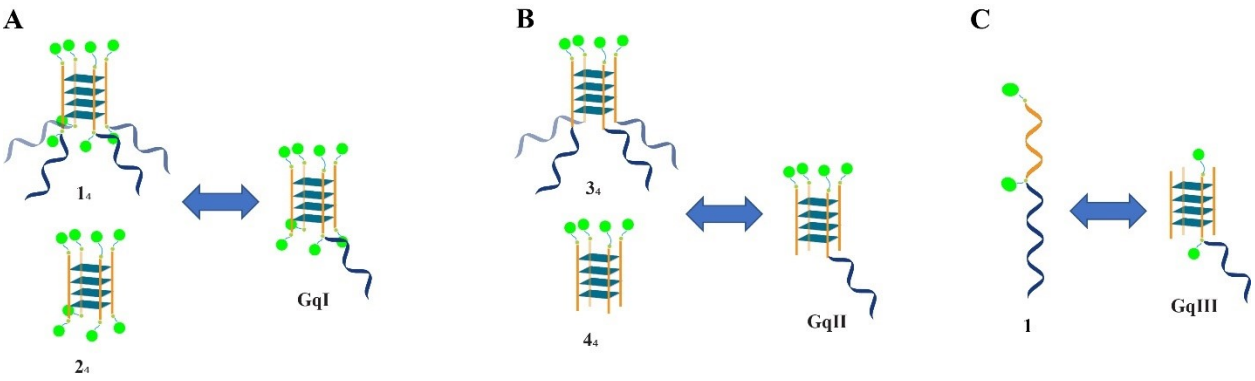

Figure S6. Scheme showing the homomeric quadruplex assemblies and single-strands used to estimate the quantum yield values of the heteromeric assemblies **GqI-GqIII**.

S3.2. Quantum yield calculation procedure

Fluorescence quantum yield was determined using a PTI Quantamaster spectrophotometer equipped with a red sensitive Hamamatsu R928 PMT detector. All samples were measured in an appropriate buffer (K^+ buffer for G-quadruplexes and 100 mM LiCl solution for single strands since it is known to inhibit quadruplex formation) using the standard reference 6-FAM dye. The reported fluorescence quantum yield value for 6-FAM dye is 0.75 [1]. The excitation wavelength was chosen by tallying the closely matching absorption values of 6-FAM dye and fluorescein conjugated ODNs in the UV-vis absorption profiles. At 494 nm, all sample solutions UV-vis absorption were closely matched (Figure S7). The corresponding integrated emissions were calculated from the emission profiles (Figure S8). The following equation was used for the relative fluorescence quantum yield measurements (Table S1). [2], [3]

$$\emptyset_x = \emptyset_{st}\left(\frac{F_x}{F_{st}}\right)\left(\frac{f_{st}}{f_x}\right)\left(\frac{\eta_x^2}{\eta_{st}^2}\right)$$ (eq. S7)

Where, $\emptyset_x$ and $\emptyset_{st}$ denote quantum yield for the unknown and the standard respectively. Similarly, F_x and F_{st} denote the integrated fluorescence intensity, f_x and f_{st} denote the absorption factor [$f = 1\text{-}10^{-A}$, where

A is the absorbance values at the excitation wavelength], and η_x and η_{st} denote the refractive index of the solvent systems.

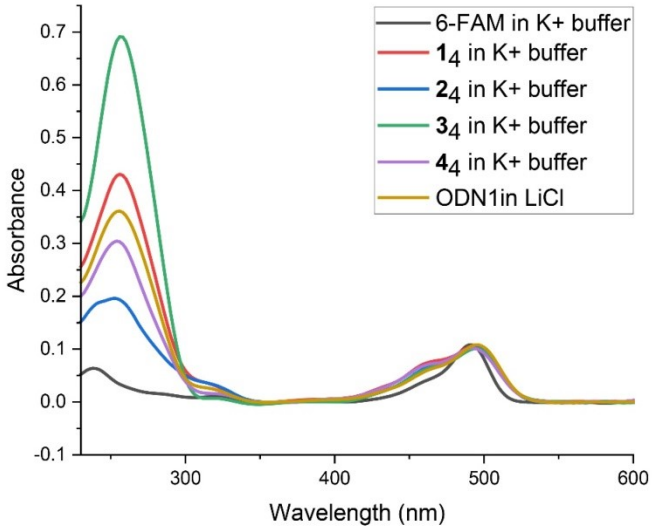

Figure S7. UV-vis. profile of all samples with absorption intensity matched at 494 nm. **Black:** 6-FAM in K^+ buffer. **Red:** $\mathbf{1}_4$ in K^+ buffer. **Blue:** $\mathbf{2}_4$ in K+ buffer. **Green:** $\mathbf{3}_4$ in K+ buffer. **Purple:** $\mathbf{4}_4$ in K+ buffer. **Yellow:** ODN1 in 100 mM LiCl.

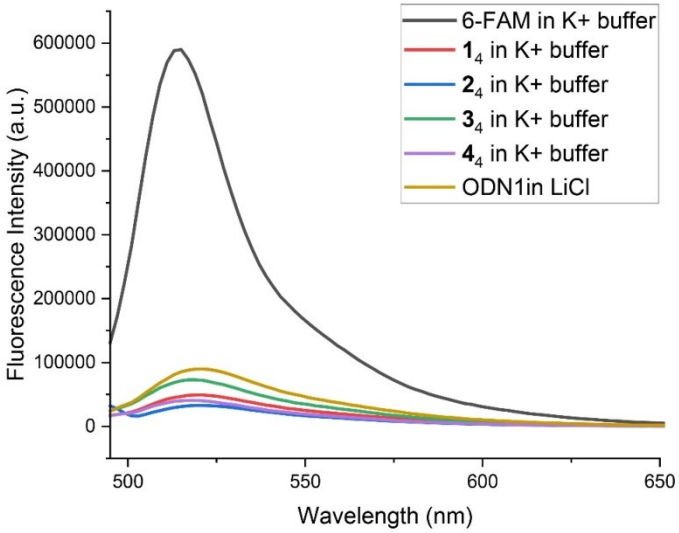

Figure S8. Fluorescence emission profile of all samples corresponding to samples with absorption matched excitation at 494 nm. **Black:** 6-FAM in K^+ buffer. **Red:** $\mathbf{1}_4$ in K^+ buffer. **Blue:** $\mathbf{2}_4$ in K+ buffer. **Green:** $\mathbf{3}_4$ in K+ buffer. **Purple:** $\mathbf{4}_4$ in K+ buffer. **Yellow:** ODN1 in 100 mM LiCl.

Table S1. Parameters for estimating quantum yield values for **GqI-GqIII**.

System	Absorption (494 nm)	f = 1-10^{-A}	F x 10^{-7} (495-650 nm)	$\frac{\eta_x^2}{\eta_{st}^2}$	QY
6-FAM	0.105	0.215	2.48	1	0.75

1_4	0.107	0.218	0.28	1	0.083
2_4	0.103	0.211	0.19	1	0.059
3_4	0.101	0.207	0.40	1	0.125
4_4	0.102	0.211	0.22	1	0.068
1	0.108	0.220	0.51	1	0.150
GqI	-	-	-	-	0.065
GqII	-	-	-	-	0.082
GqIII	-	-	-	-	0.150

Table S1 summarizes the quantum yield estimations for all assemblies. The quantum yield for all 3 assemblies is in a relatively close range (from 0.07 for **GqI** to 0.15 for **GqIII)**. As expected, the overall quantum yield of heteromeric assemblies is lower than the quantum yield of 6-carbxoyfluorescein dye reference [1] due to the environment differences (π-π stacking of neighboring fluorophores and the proximity to guanine nucleobases) [4].

S4. Photophysical Studies

All steady-state fluorescence experiments were carried out using Multimode Reader by applying 50 µL sample in Costar- 96 well standard black plates.

S4.1. Overall FRET efficiency (*E*)

The experimental overall FRET efficiency (*E*) from steady-state fluorescence study was calculated based on the donors' emission quenching in presence of acceptor dye by equation S8.[5], [6]

$$E = 1 - \frac{I_{DA,520}}{I_{D,520}} \qquad \text{(eq. S8)}$$

Where $I_{DA,520}$ and $I_{D,520}$ are fluorescence intensity of donor at 520 nm in the presence and absence of acceptor dye, respectively. The donor was excited at 490 nm.

S4.2. Antennae effect (*AE*)

In addition, the antenna effect of the light harvesting systems was calculated based on equation S9.[7], [8]

$$AE = \frac{I_{DA,\,490} - I_{A,490}}{I_{A,\,535}} \qquad \text{(eq. S9)}$$

Where $I_{DA,490}$ is the intensity of acceptor (TAMRA) emission (at 580 nm) when the exciting complex contains donors (excited at 490 nm), $I_{A,490}$ is the intensity of acceptor emission when the acceptor only (without any donors) is excited at 490 nm, and $I_{A,\,535}$ is the acceptor emission at 580 nm when donor-

acceptor complex is directly excited at the acceptor excitation wavelength at 535 nm (TAMRA absorption).

S4.3. Effective absorption coefficient (ε_{eff})

Finally, the effective absorption coefficient (ε_{eff}) was calculated based on equation S10 by multiplying the antenna effect (*AE*) and absorption coefficient of acceptor dye ($\varepsilon_{TAMRA\text{-}535\ nm}$: 54000 L. mole^{-1}·cm^{-1} from AATbio.com). The ε_{eff} provides the apparent absorption coefficient of the acceptor at the excitation wavelength of the donor. Further, this parameter can be used to compare different systems with different donors and acceptors.[8]

$$\varepsilon_{eff} = AE \times \varepsilon_A\,(M^{-1}\,cm^{-1}) \qquad \text{(eq. S10)}$$

S5. Supplementary Tables

Table S2. The sequence of ODNs used in this study and calculated maximum absorption coefficients.

ODN strand name	Sequence (5' - 3')	*Max. absorption coefficient at 260 nm ($L.mole^{-1} \cdot cm^{-1}$)
ODN1 or **1**	6-FAM-TGG GGG AT^{FAM}A GCT GAG GTC ACG TTA	274560
ODN2 or **2**	6-FAM-TGG GGG AT^{FAM}	115160
ODN3 or **3**	6-FAM-TGG GGG ATA GCT GAG GTC ACG TTA	260860
ODN4 or **4**	6-FAM-TGG GGG AT	101460
ODN5 or **5**	TGG GGG AT	80500
TAM-ODN or EA	TAA CGT GAC CT^{TAM}C AGC TAT	201100

*All Maximum absorption coefficients of ODNs and dyes were obtained from IDT-DNA.

Table S3. RP-HPLC gradient used for ODN purification.

Time (min)	Flow rate (ml/min)	Solvent A%	Solvent B%
0.00	0.75	100	0
0.01	1.00	100	0
2.50	1.00	100	0
12.50	1.00	92	8
25.00	1.00	80	20
34.00	1.00	50	50
36.00	1.00	0	100
38.00	1.00	0	100
40.00	1.00	100	0
42.00	1.00	100	0

S6. Supplementary figures

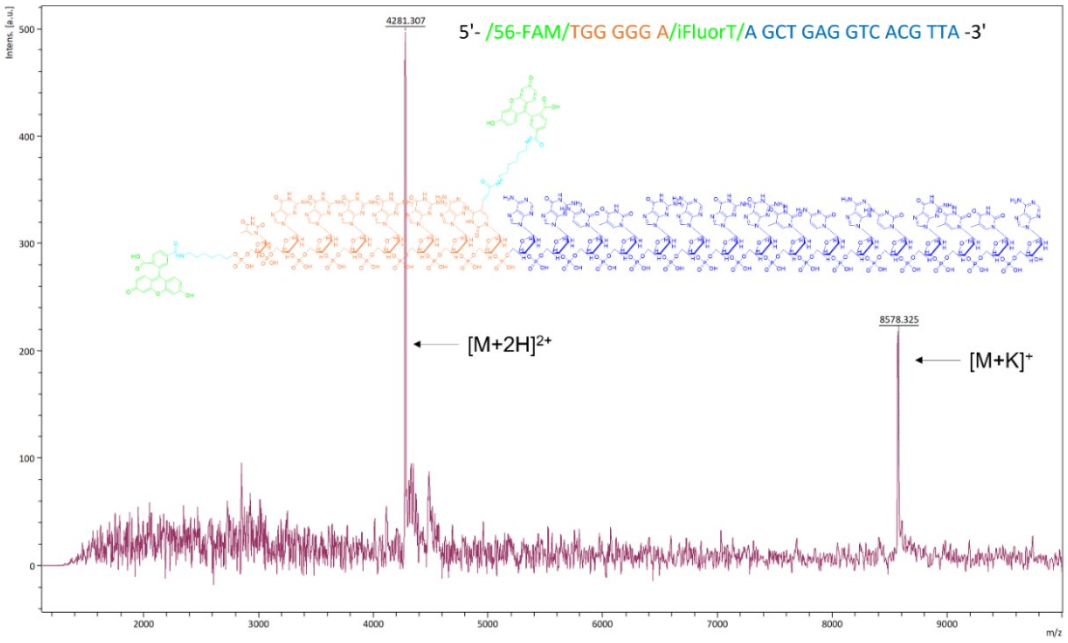

Figure S9. MALDI-TOF MS spectra of ODN1; observed MW: 8578.32 Da, calculated MW: 8577.86 Da for $[M+K]^+$.

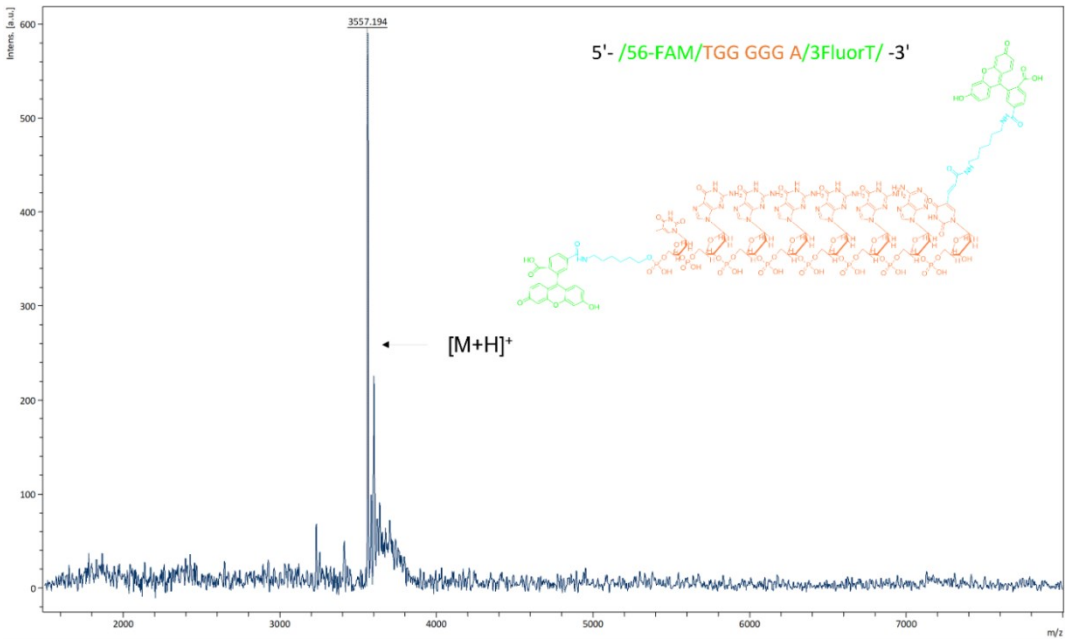

Figure S10. MALDI-TOF MS spectra of ODN2, observed MW:3557.19 Da, calculated MW: 3556.71 Da for $[M+H]^+$.

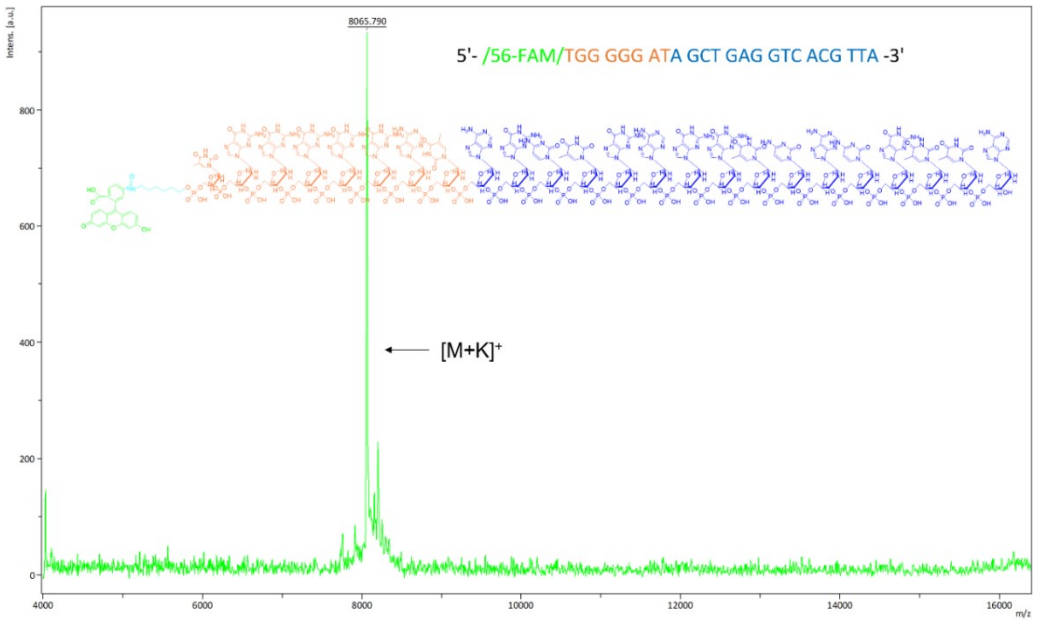

Figure S11. MALDI-TOF MS spectra of ODN3; observed MW: 8065.79 Da, calculated MW: 8065.36 Da for $[M+K]^+$.

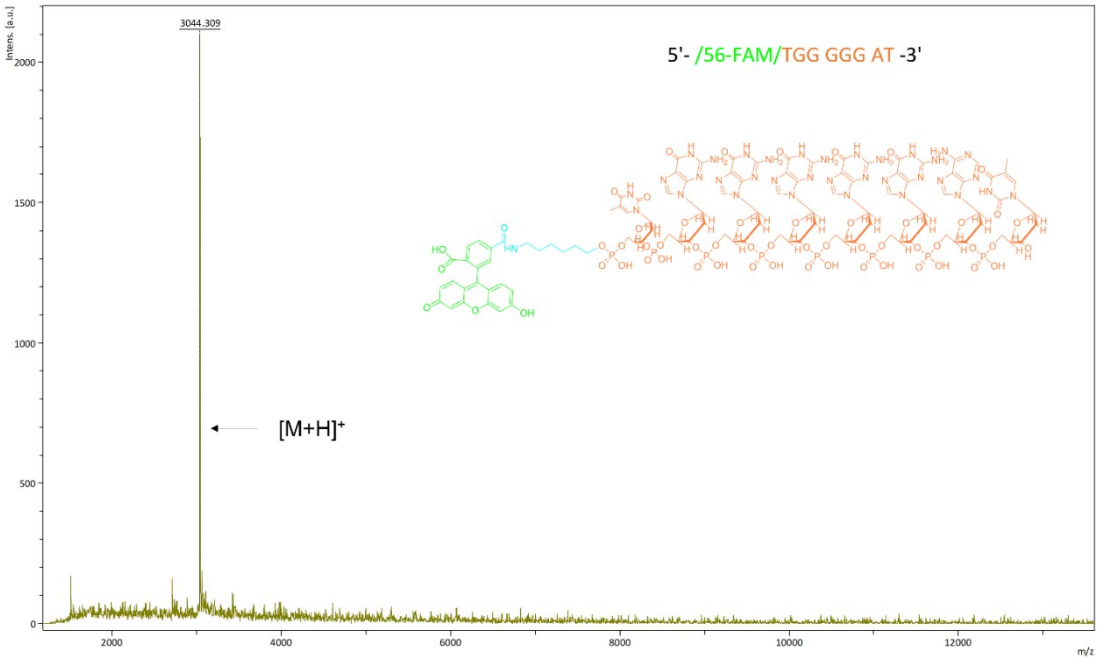

Figure S12. MALDI-TOF MS spectra of ODN4; observed MW: 3044.31Da, calculated MW: 3044.11 Da for $[M+H]^+$.

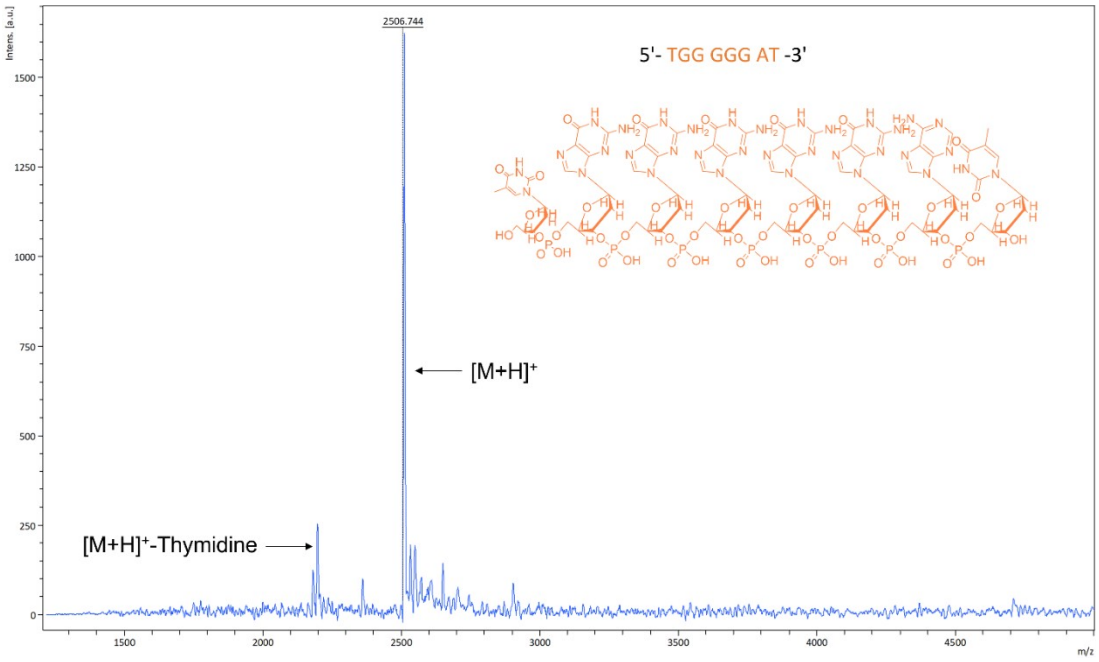

Figure S13. MALDI-TOF MS spectra of ODN5; observed MW: 2506.74 Da, calculated MW: 2506.71Da for $[M+H]^+$.

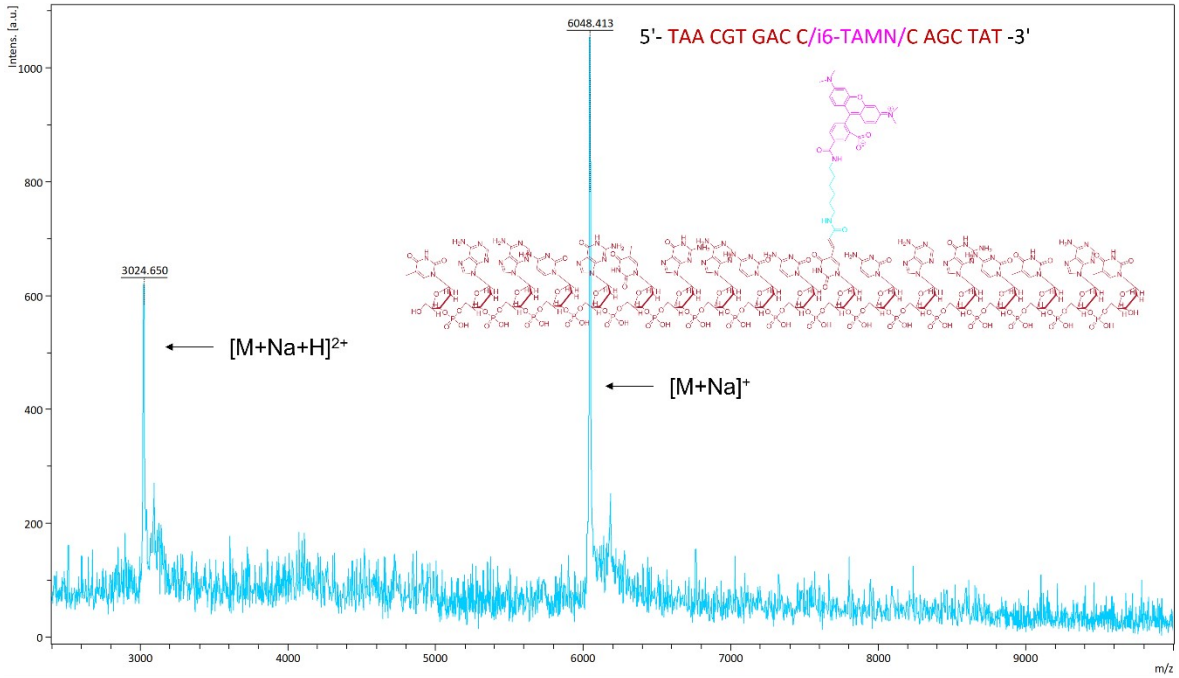

Figure14. MALDI-TOF MS spectra of TAMRA-ODN (EA strand); observed MW: 6048.13 Da, calculated MW: 6048.29 Da for $[M+Na]^+$.

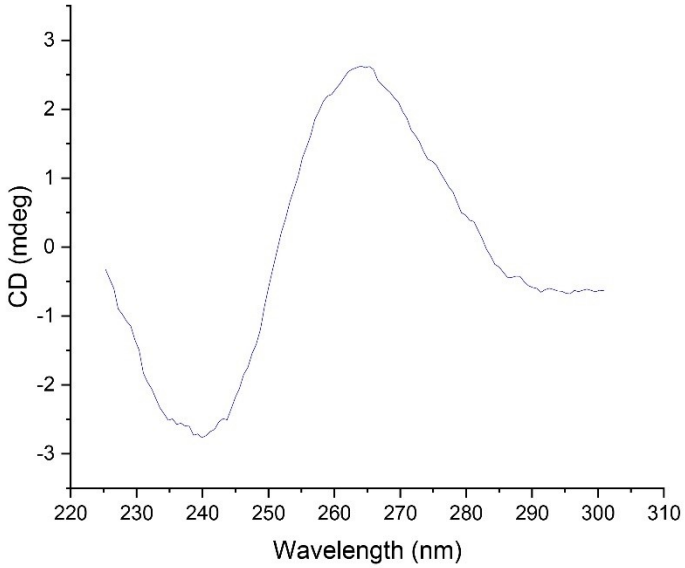

Figure S15. CD spectrum of self-assembled ODNs **3** and **4** (20 μM). Data were smoothed by applying a Savitzky-Golay filter.

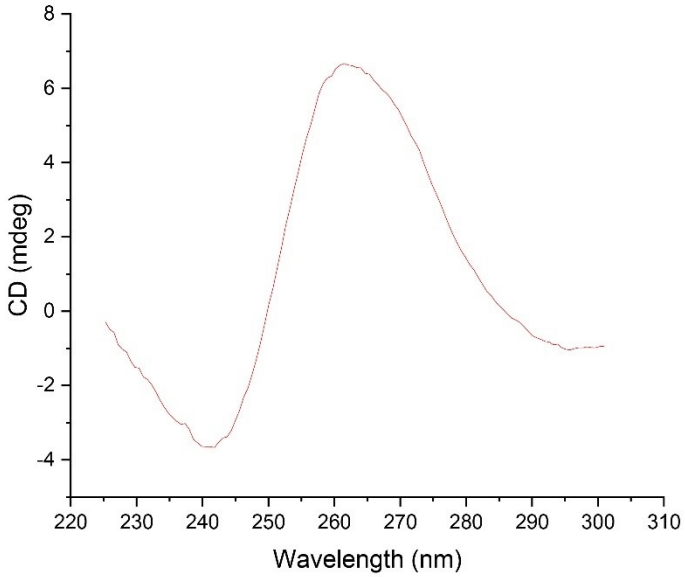

Figure S16. CD spectrum of self-assembled ODNs **1** and **5** (20 μM). Data were smoothed by applying a Savitzky-Golay filter.

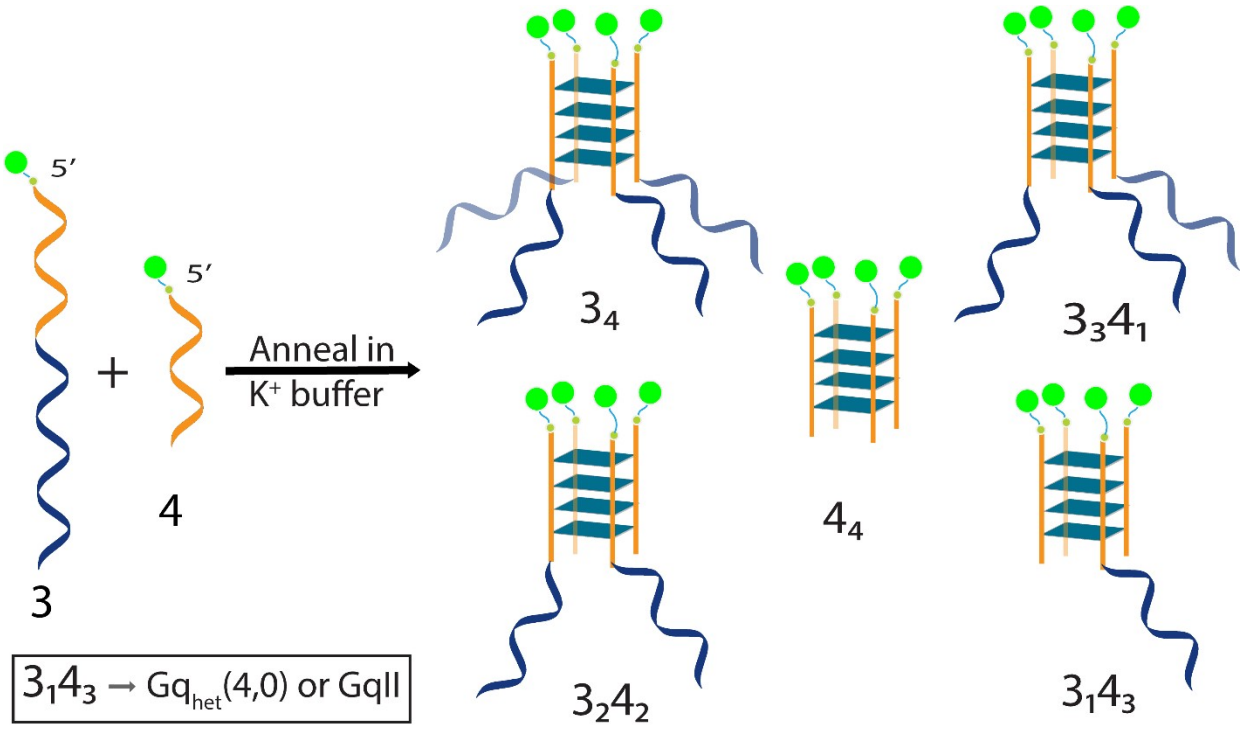

Figure S17. Schematic presentation of **GqII** ($\mathbf{3_14_3}$) formation upon equimolar mixing of ODNs **3** and **4**.

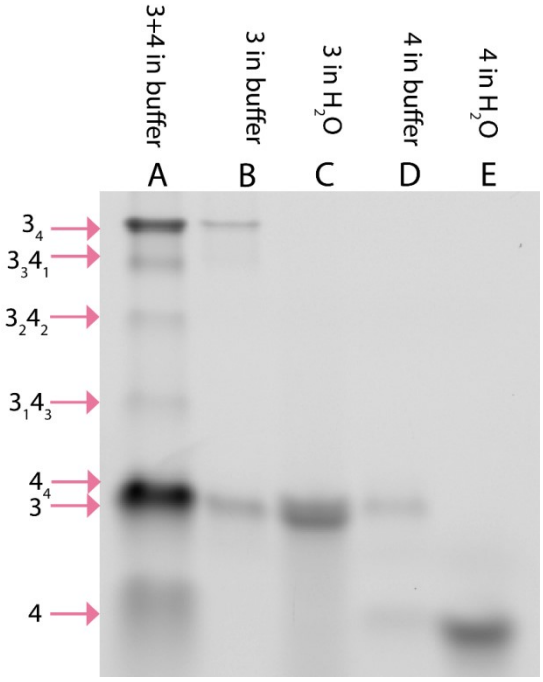

Figure S18. PAGE studies to identify **GqII** ($\mathbf{3_14_3}$): **lane A.** self-assembly of ODNs **3** and **4** in K⁺ buffer, **lane B.** ODN **3** in K⁺ buffer, **lane C**. ODN **3** in deionized water, **lane D**. ODN **4** in K⁺ buffer, and **lane E**. ODN **4** in deionized water). Note the concentrations loaded on lane A (50 μM per ODN) is 10x more than for the control lanes. Gel electrophoresis was performed in TBA buffer containing 33 mM KCl.

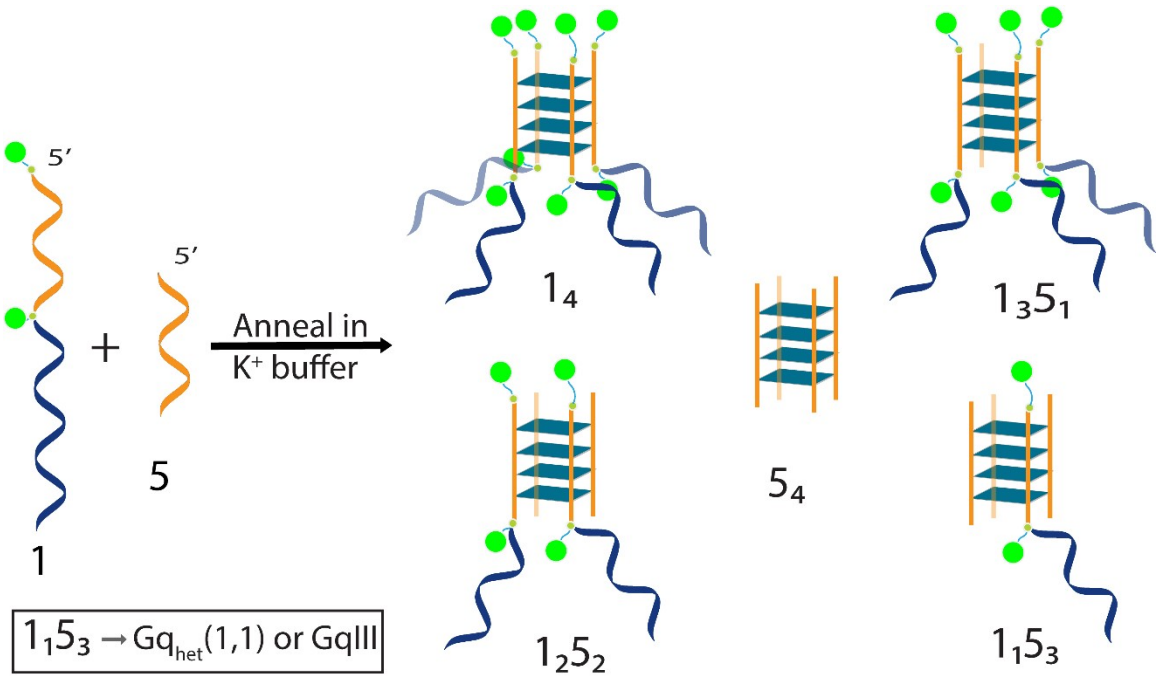

Figure S19. Schematic presentation of **GqIII** (**1**$_1$**5**$_3$) formation upon equimolar mixing of ODNs **1** and **5**.

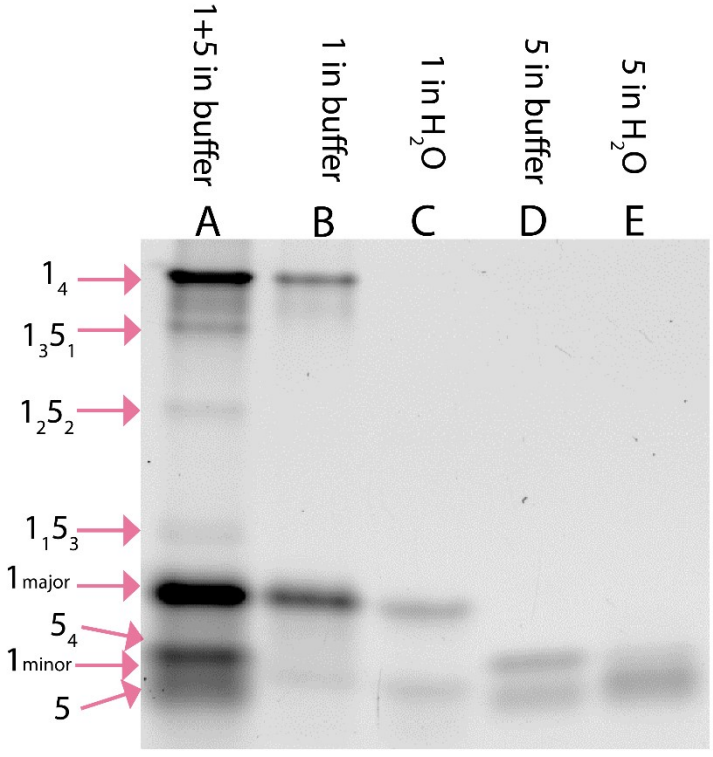

Figure S20. PAGE studies to identify **GqIII** (**1**$_1$**5**$_3$): **lane A.** self-assembly of ODNs **1** and **5** in K⁺ buffer, **lane B.** ODN **1** in K⁺ buffer, **lane C**. ODN **1** in deionized water, **lane D**. ODN **5** in K⁺ buffer, and **lane E**. ODN **5** in deionized water). Note the concentrations loaded on lane A (50 μM per ODN) is 10x more than for the control lanes. Gel electrophoresis was performed in TBE buffer containing 33 mM KCl.

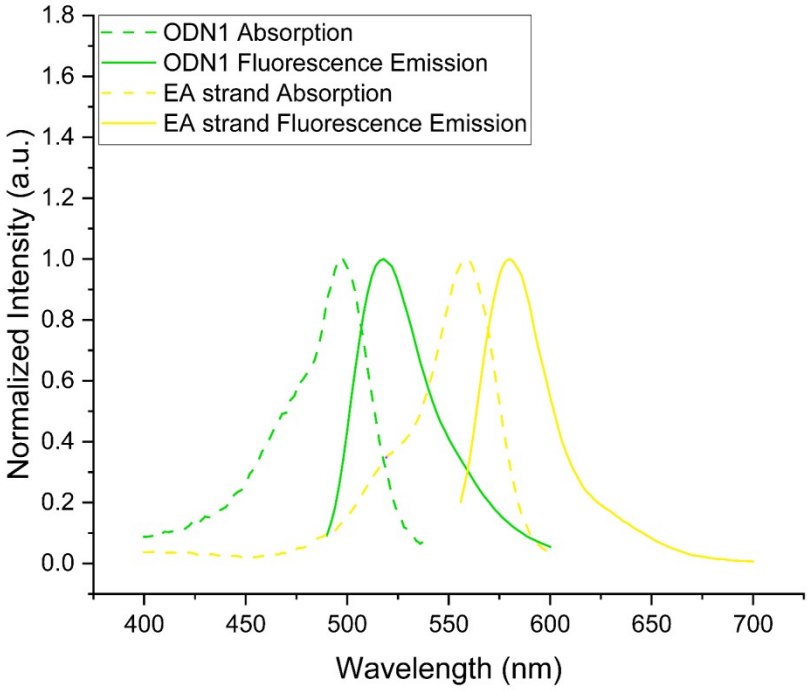

Figure S21. Energy level matching between donor dyes (Fluorescein) on ODN1 and acceptor dye (TAMRA) on EA strand.

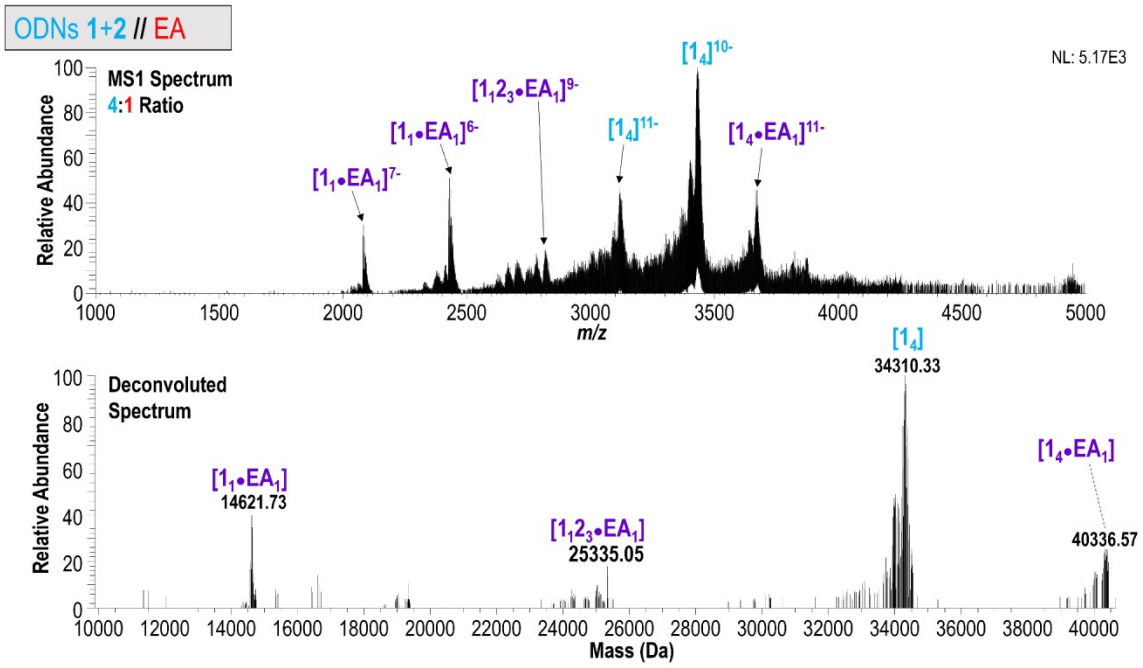

Figure S22. ESI-MS analysis of ODNs **1**+**2**:**EA** complex (4:1 ratio). **Upper)** MS1 and **Lower)** deconvoluted mass spectrum of ODNs **1**+**2**:**EA** complex in 150 mM ammonium acetate. Note: Observed mass for $\mathbf{1}_1\mathbf{2}_3$:**EA** (or **GqI**:**EA**) is 25.3 kDa.

References

[1] X. F. Zhang, J. Zhang, and L. Liu, 'Fluorescence properties of twenty fluorescein derivatives: Lifetime, quantum yield, absorption and emission spectra', *J Fluoresc*, vol. 24, no. 3, pp. 819–826, 2014, doi: 10.1007/s10895-014-1356-5.

[2] P. Pathak *et al.*, 'Bright G-Quadruplex Nanostructures Functionalized with Porphyrin Lanterns', *J Am Chem Soc*, vol. 141, no. 32, pp. 12582–12591, Aug. 2019, doi: 10.1021/jacs.9b03250.

[3] C. Würth, M. Grabolle, J. Pauli, M. Spieles, and U. Resch-Genger, 'Relative and absolute determination of fluorescence quantum yields of transparent samples', *Nat Protoc*, vol. 8, no. 8, pp. 1535–1550, 2013, doi: 10.1038/nprot.2013.087.

[4] J. Lietard, D. Ameur, and M. M. Somoza, 'Sequence-dependent quenching of fluorescein fluorescence on single-stranded and double-stranded DNA', *RSC Adv*, vol. 12, no. 9, pp. 5629–5637, Feb. 2022, doi: 10.1039/d2ra00534d.

[5] H. Kashida, H. Azuma, R. Maruyama, Y. Araki, T. Wada, and H. Asanuma, 'Efficient Light-Harvesting Antennae Resulting from the Dense Organization of Dyes into DNA Junctions through d-Threoninol', *Angewandte Chemie - International Edition*, vol. 59, no. 28, pp. 11360–11363, Jul. 2020, doi: 10.1002/anie.202004221.

[6] S. Hirashima, H. Sugiyama, and S. Park, 'Construction of a FRET System in a Double-Stranded DNA Using Fluorescent Thymidine and Cytidine Analogs', *Journal of Physical Chemistry B*, vol. 124, no. 40, pp. 8794–8800, Oct. 2020, doi: 10.1021/acs.jpcb.0c06879.

[7] L. Olejko and I. Bald, 'FRET efficiency and antenna effect in multi-color DNA origami-based light harvesting systems', *RSC Adv*, vol. 7, no. 39, pp. 23924–23934, 2017, doi: 10.1039/c7ra02114c.

[8] J. G. Woller, J. K. Hannestad, and B. Albinsson, 'Self-assembled nanoscale DNA-porphyrin complex for artificial light harvesting', *J Am Chem Soc*, vol. 135, no. 7, pp. 2759–2768, Feb. 2013, doi: 10.1021/ja311828v.